A Fast On-Board Relative Positioning Module for Multi-Robot Systems

Jim Pugh, *Student Member, IEEE*, Xavier Raemy, Cédric Favre, Riccardo Falconi, and Alcherio Martinoli, *Member, IEEE*

***Abstract*—We present an on-board robotic module which can determine relative positions among miniature robots. The module uses high-frequency modulated infrared emissions to enable nearby robots to determine the range, bearing, and message of the sender with a rapid update rate. A CSMA protocol is employed for scalable operation. We describe a technique for calculating the range and bearing between robots, which can be generalized for use with more sophisticated relative positioning systems. Using this method, we characterize the accuracy of positioning between robots and identify different sources of imprecision. Finally, the utility of this module is clearly demonstrated with several robotic formation experiments, where precise multi-robot formations are maintained throughout difficult maneuvers.**

I. Introduction

Multi-robot systems is an emerging field which has recently drawn the attention of the robotics community. Multi-robot systems offer considerable advantages in comparison to single unit systems: simultaneous sensing and acting in physically different positions, reconfigurability of the system, redundancy, sometimes even the ability to achieve superlinear performances via division of labor. For several tasks such as distributed search [13], distributed coverage [6], and movement in formation [8], knowledge of a robot's own location and/or that of neighboring teammates is required.

Artificial localization systems can be roughly classified into two main categories: absolute and relative positioning systems. Absolute localization determines position in a global coordinate framework; examples include GPS-like solutions (also available for indoor environments, see for instance [20]) and external monitoring solutions, such as an overhead camera system (for instance [15]). For certain types of tasks, only relative distance and bearing information is needed. While this information could also be obtained with an absolute positioning system and an effective communication channel, the communication overhead resulting from this solution might be much higher and less scalable than a solution based on a relative localization system. In addition, certain situations do not allow for effective global localization (e.g., a distributed system in an unknown environment in which no GPS reception is possible). Currently, very few relative localization systems exist that can accomplish accurate and fully scalable performance and even fewer rely only on unsophisticated hardware.

This work has been done within the Distributed Intelligent Systems and Algorithms Laboratory, École Polytechnique Fédérale de Lausanne, 1015 Lausanne, Switzerland {firstname.lastname}@epfl.ch

Among tasks that require robotic localization, accurate formation movement is one of the most difficult. Maintaining precise relative positions in a moving group of robots is only possible with fast and accurate positional updates. This strongly motivates the development of effective localization technology, as formation movement is an integral aspect of many multi-robot applications. Common examples include control of Unmanned Air Vehicles (UAVs), collective transport of heavy/large objects, maintaining safe positions in an automated traffic system, and guaranteeing good sensor coverage for tasks such as search and rescue missions.

In this work, we present a newly developed on-board relative positioning module for miniature mobile robots which offers fast and accurate performance; we demonstrate the effectiveness of this module in several multi-robot formation experiments. Section II of this paper provides some background on multi-robot relative positioning and formation movement. In Section III, we describe the technological design of our module. A method for determining the range and bearing between robots using the module is presented in Section IV. In Section V, we characterize the capabilities and accuracy of the system. Section VI describes several multi-robot formation experiments where the relative positioning module enables effective performance. In Section VII, we discuss the implications of our results and suggest directions for future work, and Section VIII concludes.

II. Background

Although it is necessary for many multi-robot applications, there has been relatively little research done on development of on-board relative positioning systems for miniature robots. Several contributions have explored using sophisticated hardware, such as laser range finders and cameras, to achieve inter-robot positioning (e.g., [9], [14], [24]). However, these solutions tend to be economically, computationally, and energetically expensive, which is not ideal for large swarms of simple, cheap robots.

A more low-cost technique for relative positioning is to use modulated infrared signals emissions; receiving robots can compare the Received Signal Strength Indication (RSSI) from multiple sensors in order to gauge the range and bearing of the emitter robot (in this case, RSSI refers to the power present in a received infrared signal, as opposed to its more common usage for the power present in a received radio signal). This type of system was presented and characterized by Kelly and Martinoli [16] and Pugh and Martinoli [22]; the system

had a maximum range of 3 m, with a maximum distance error of 8% of range and a maximum bearing error of 17.4° (7.00° on average). The system was also capable of encoding small amounts of data in emissions which could be used for robot identification. Another infrared-based system presented by McLurkin and Smith [21] achieved good performance at close range (error of 1 cm in range and 2° in bearing at a range of 30 cm), but has a maximum range of 250 cm, and a smaller, unspecified maximum range that provides reliable positioning. An infrared-based solution using an embedded array of 256 photodiodes is currently being developed by Bergbreiter et al. [3], which could potentially offer quite high accuracy in both range and bearing for very small robotic platforms.

Using infrared as a medium for sending relative positioning signals has various costs and benefits. Infrared signals have the potential to be very fast, with the signal duration potentially being on the order of microseconds, which could allow for very fast update rates and fast communication. Infrared transceivers could also be produced at a very small scale, allowing the same concepts to be used for future micro-robots. However, using RSSI to calculate range and bearing leaves the system susceptive to interference from external signals, which might limit the accuracy and make the system difficult to use outdoors. The emitters and receivers are also very sensitive to miscalibration for the same reason. Finally, infrared light can be occluded if a robot or some other obstacle gets in the way, which could prevent the signal from accurately reaching other robots; this could, however, actually be a benefit in some scenarios, where robots need to know whether or not they are in line-of-sight of each other.

An alternative low-cost technique for relative positioning is to use synchronized ultrasonic and radio emissions to signal other robots; by comparing the arrival times of the radio and ultrasonic signals on multiple microphones, a receiving robot can deduce the range and bearing of the emitting robot using the time-of-flight of sound. Using this type of system, Bisson et al. achieved average bearing error of 1.84° and average range error of 0.375 cm up to a range of 810 cm [4] and Rivard et al. later used a similar system for formation movement with four robots [25]. Time-of-flight accuracy constraints make it difficult to create very small ultrasonic systems for use with miniature robotic platforms however; Rivard et al. [25] found that reducing the size of the system by a factor n increased bearing error by approximately the same factor. This suggests that adapting their system designed for Pioneer 2 robots (with a diameter of approximately 30 cm, which is considerably larger than the infrared-based systems mentioned previously) for miniature robotic platforms would lead to a significant increase in bearing error.

As is shown by Bisson and Rivard's results, ultrasonic-based relative positioning can be very accurate, especially over longer ranges. Because RSSI is not used to calculate range and bearing, the transceivers do not need to be carefully calibrated for the system to work. Ultrasound is also better able to pass through solid objects than infrared, making ultrasound systems less sensitive to occlusion. A problem with ultrasound is that signals are slow to dissipate, especially in enclosed environments. This limits the rate at which robots could transmit signals, especially as the number of robots increases; in the work of Rivard et al. [25], the transmission rate for a robot was $\frac{1}{0.075N}$ Hz for N robots, which means that with 14 or more robots the update rate would be less than 1 Hz. Crosstalk between ultrasonic sensors and reflections is a known problem for proximity sensing, and this effect caused problems with the system used by Grabowski and Khosla [10].

A recent method of positioning which has not yet been adapted for use with mobile robots is using radio signals with time-of-flight and phased array reception. By sending radio messages back and forth and accurately measuring the times of transmission and arrival, it is possible to measure the range between robots (for example, see [17] and [19]), and bearing can be calculated by comparing the phases of received signals on multiple receivers (see [12] for example). Radio localization can be used over much longer ranges than infrared or ultrasound, is not sensitive to miscalibration since it uses time-of-flight, and is not very sensitive to occlusion. However, it is difficult to very accurately measure signal arrival times, and therefore current radio localization techniques tend to have errors on the order of several tens of centimeters or higher. This is too large for small-scale robot systems and certainly too large for micro-robots. Future improvements in the technology may allow this problem to be overcome.

There has been a substantial amount of research on robotic formation movement in recent years. However, the majority of work has been restricted to analysis and simulation (for example, [2], [5], [7], [28], [29]). Only a few studies have actually tested their algorithms on real robots. In [1], motor schemas were used in simulation and with Nomad 150 robots to allow two robots to navigate in formation while avoiding obstacles. An algorithm was developed for formation movement in [8] and implemented in simulation as well as with four real Pioneer2 robots in a variety of different dynamic formations. In [18], several formation control strategies based on simulated relative positioning were proposed, analyzed, and tested on a group of three custom robots. An algorithm for formation movement planning was developed and analyzed in [11] and tested on three Magellan Pro robots. Several simple formation methods were tested on four Moorebot robots in [23]. In [26], a physics-based technique for controlling a robot swarm was proposed, analyzed, and tested on seven custom real robots. Several different formations were tested using the ultrasound-based relative positioning system from [25].

Of the previous studies on robotic formation movement using real robots, all except for [8], [23], [26], and [25] simulated relative positioning within the formation using some sort of global positioning system. While the experiments in [8] did use an on-board relative positioning system, this system used both a laser range-finder and a mobile camera, and would therefore be infeasible for use on low-cost, miniature robots. The experiments in [23] used the simple, infrared-based, on-board module described by Pugh and Martinoli [22]. This system achieved mediocre formation performance with real robots, although simulations suggested that it could be significantly improved with a faster positioning update rate (going from the 2 Hz update rate of the real system to 16 Hz). In [26], infrared-proximity sensors were used to determine the

approximate range and bearings of nearby robots; while the system was effective for the experiment presented in the work, it would be very suspectible to interference from any other obstacles (including other robots) and not appropriate for general experiments. Movement with several different formations was achieved in [25] using their on-board ultrasound-based relative positioning system.

The relative positioning module we use in this work is an infrared-based system. While it cannot achieve accuracy comparable to existing ultrasound-based solutions, the system accuracy is as good or better than previous infrared-based designs, and significantly better than radio-based solutions. The update rate of the system is also substantially better than previous infrared- and ultrasound-based designs, making it suitable for fast, accurate formation control.

III. Module Design

The relative positioning board described here is based on the system described in [16]. This was an infrared-based system with four photo-diode receivers that was used by the Moorebot platform [27]; the system had a bearing accuracy of 45°, a range accuracy of 40 cm, and an update rate of 2 Hz for ten robots operating simultaneously. Our new design attempts to overcome many of the shortcomings that were present in the previous model.

A. Robotic Platform

Our relative positioning module is designed for the newly developed Khepera III robotic platform (see Fig. 1), produced by K-Team Corporation with development assistance from our laboratory. The robot has a diameter of 12 cm, making it appropriate for multi-robot indoor experimentation. Locomotion is accomplished via a differential drive system using two independent motors. The Khepera III uses the Korebot platform, running a standard embedded Linux operating system on an Intel XSCALE PXA-255 processor running at 400 MHz. Belts of both ultrasonic and infrared proximity sensors surround the robot, allowing for detection of both close and medium range objects. The robot can be endowed with IEEE 802.11 wireless ability by using an appropriate card with the built-in CompactFlash slot. A stackable expansion bus on top of the robot allows for the addition of custom robot modules, which is how our relative positioning boards are connected.

The module from [16] was designed for the Moorebot robotic platform and mounted via a PC/104 stack. This stack was not centered on the robot, however, which resulted in inaccuracies in both range and bearing measurements. Our new module is centered on the Khepera III robots, removing this source of errors.

B. Hardware Design

Our relative positioning system is designed using only off-the-shelf electrical components, reducing module cost and increasing ease of replication. In order to encode and decode modulated signals, standard radio frequency (RF) hardware is used for frequency modulation (FM) and demodulation. The

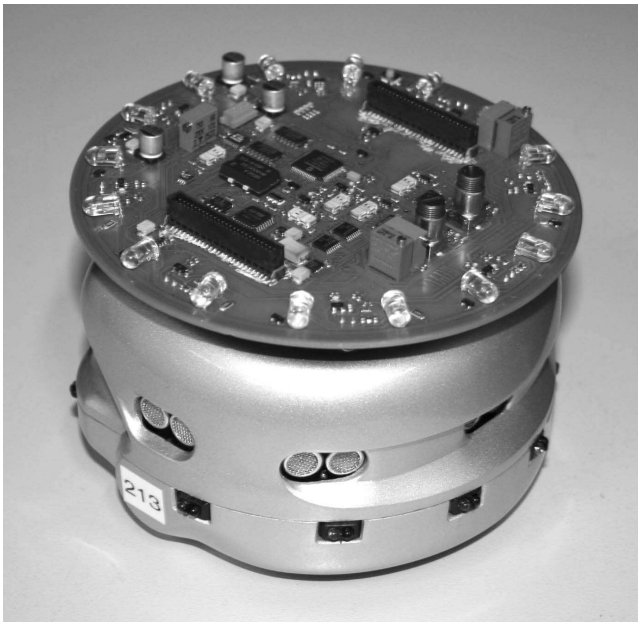

Fig. 1. Khepera III robot with relative positioning module attached

module uses a dedicated 16-bit dsPIC33F processor running at 40 MIPS for all module control and signal processing. Sixteen evenly-spaced infrared Light Emitting Diodes (LEDs) divided into eight independently controllable sectors can emit the modulated signal with up to 360° coverage. Emission power can be set to three different levels depending upon the desired range of operation, with a maximum transmission range of approximately 330 cm. Infrared signals from other modules can be received on eight evenly-spaced infrared photo-diodes. These diodes are connected via a multiplexer to an RF demodulator, which can extract both the RSSI and encoded data from the signal.

In the system from [16], a modulation frequency of 455 KHz was used for the infrared transmission. This limited the rate of data encoding in the signal to 2 Kbits/s. In our system, we use a modulation frequency of 10.7 MHz, more than a full order of magnitude higher than the previous system. While this makes hardware component selection and printed circuit routing somewhat more difficult, it allows us to send data much more quickly at 20 Kbits/s.

C. Communication Protocol

In order to schedule the transmission of infrared packets between robots, we employ a Carrier Sense Multiple Access (CSMA) communication protocol. When a robot wants to send a packet, it “listens” to see if it detects any other robot already transmitting. If someone else is sending, the robot waits until the transmission is complete before trying again. If not, it begins broadcasting with its infrared LEDs to signal nearby robots that it is ready to send a packet. After a randomized length of time (between 100 and 150 microseconds), the robot disables its broadcast and again checks whether any other robot is transmitting; this allows two robots who begin transmitting simultaneously to detect that there has been a

"collision" between their emissions. If no other signal is detected, the robot once again begins broadcasting, now encoding data in its transmission. Data is comprised of 2 start bits (1 followed by 0), 16 bits of packet message contents, 4 bits of message checksum, and 2 end bits (1 followed by 0). After data transmission is complete, transmission continues (sending a 0-bit signal) for 400 microseconds to allow for RSSI measurements, then ceases. The total packet length is approximately 1.9 milliseconds (as opposed to 17 ms in [16]). For a visual depiction of the packet, see Fig. 2.

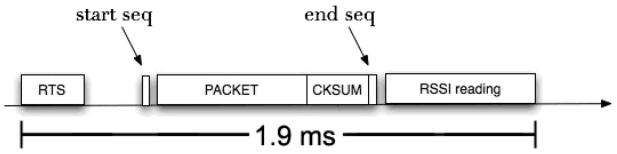

Fig. 2. Relative positioning packet contents

For repeated transmissions, in order to determine the delay time until the next packet broadcast, robots use adaptive randomized backoff times. Once a transmission has been completed, a robot will choose a countdown value until the next transmission. The countdown value is uniformly selected between 1 and BACKOFF_MAX and is decremented every microsecond when no transmission is occuring. Initially, BACKOFF_MAX is set to 30. In the event of a transmission collision, the value of BACKOFF_MAX is increased to twice its former value. In the event of a successful transmission, BACKOFF_MAX is lowered to 0.9 times its previous value, with a minimum value of 30 (i.e. minimum backoff time is 30 microseconds). This adaptation allows the communication protocol to continue to function efficiently even with very large numbers of transmitting robots, as the inter-packet delay will scale to limit the number of collisions. Because the adaptation is done in real-time, robots may be introduced to or removed from the environment during run time, making the multi-robot system dynamically scalable.

By using faster data transmission rates and adaptive backoff times, our new system is able to operate much more quickly than the system from [16]. The previous module could potentially operate at almost 20 Hz in experiments with two robots. However, the update rate was limited to a fixed rate of 2 Hz in order to allow experiments with up to 10 robots. Our new module does not need to be limited since it can automatically adjust its rate, going from a potential maximum of 250 Hz with two robots to 25 Hz with 10 robots. However, since extremely fast update rates cannot be processed quickly enough by the robot, we manually limit the modules to transmit at a maximum rate of 30 Hz.

D. Firmware Design

The dedicated dsPIC33F processor on our relative positioning modules is programmed to control the packet emission and reception on the board, as well as to communicate with the Khepera III robot via an I^2C bus. Because RSSI and data from infrared transmissions may contain noise (especially when robots are far apart) that would cause error in relative positioning, we employ several strategies to intelligently detect and decode packets from other robots.

In order to calculate bearing, it is necessary to compare RSSI between different receivers; these receivers must be calibrated using the same baseline to get an accurate comparison. To account for variations among infrared photo-diodes on the relative positioning module, the system firmware includes an automatic baseline calibration routine which can be run when no transmissions are occurring. This routine measures both the mean and variance of the RSSI resulting from background noise on all receiver channels. The module then uses these values to calculate RSSI thresholds which reject 95% of background measurements (assuming Gaussian distributions). These thresholds are then used to determine when receiver channels are detecting a signal from a transmitting robot.

When reading the contents of a packet, our system samples the logic level of the data signal at a rate of 100 KHz. This results in five "sub-bits" per bit of the packet. To determine the value of a bit, we examine the central three sub-bits and select the value which is given by at least two of the sub-bits. This provides some level of error correction, both from potentially corrupted edge bits and from single errors within the central three sub-bits.

To determine the RSSI during a packet transmission, we exploit the fast Analog-to-Digital (A/D) converter on the dsPIC33F processor, which can operate at one million samples per second. During the RSSI reading phase on the packet, we measure the RSSI 30 times and take the average for each of the eight channels. By using this number of samples, we can eliminate much of the noise present in the signal to obtain a clean measurement of the actual signal strength.

E. Power Usage

Power consumption is a major issue for miniature mobile robots, as battery life is often very limited. It is therefore very important that Khepera III extension modules do not use excessive amounts of power to function. This is a challenge with relative positioning systems, as broadcasting to neighboring robots typically requires a considerable amount of energy.

While we have not performed systematic tests on power consumption, we have empirically observed that using the relative positioning module on the Khepera III transmitting at 30 Hz with the highest power setting decreased battery lifetime by approximately 40% from the same configuration with no relative positioning board. The module is therefore using a significant amount of the robot's energy supply. In order to partially overcome this problem, a firmware controlled power switch was included on the module, which allows the robot to shut down all relative positioning functionality except for the dsPIC processor on the board. Therefore, for experiments that only require intermittent relative positioning, the module can be kept off for most of the time and switched on only when needed, thereby dramatically reducing the average power consumption.

The voltage regulators of the relative positioning module are less sensitive to low battery voltage than the main processor

board of the Khepera III robot itself. Therefore, there is no performance degradation as battery voltage decreases, up to the point of the robot itself shutting down.

IV. Relative Positioning Algorithm

To calculate the range and bearing of a transmitting robot using the RSSI values, we employ a variation of the algorithm described by Pugh and Martinoli in [22]. The original algorithm assumed a specific angular reception strength profile for photo-diodes and aggregated the RSSI from a series of receivers to calculate an estimate of both the range and bearing of the transmitting robot. We use a very similar approach, but with a different angular reception strength profile.

The algorithm requires that receivers are evenly-spaced around the perimeter of the robot. For any received transmission, approximately half these sensors will detect the signal. We can define a "sector of interest" as some sector of n sensors with the highest received signal, where n is at most half of the total sensors. We now only need to calculate the angle offset (θ) from the center of this sector to find the bearing of the transmitting robot (ϕ).

Upon measuring the signal intensity at the individual receivers for different receiver orientations, we discovered that the intensity is closely modeled by:

$$r' = r\cos(\theta)$$

where r, which we will call the range term, would be the signal intensity at a receiver which is directly facing the transmitting robot. Let us define $m = \lfloor \frac{n}{2} \rfloor$ as the number of sensors in one half of the receiving sector. Let $r'_{-1}, ..., r'_{-m}$ be values of the sensors which have a lesser angle than the center of the receiving sector, $r'_1, ..., r'_m$ be the values of the sensors which have a greater angle than the center of the receiving sector (with r_0 as the value of the center sensor if n is odd), and β_i be the angular offset of sensor i from the sector center (for a visual depiction of an example module with $n = 3$ and $m = 1$, see Fig. 3). The value r'_i is given by:

$$r'_i = r\cos(\theta - \beta) \quad \text{with} \quad \beta_i = -\beta_{-i}$$

Therefore:

$$\begin{aligned} r'_i + r'_{-i} &= r\cos(\theta - \beta_i) + r\cos(\theta + \beta_i) \\ &= 2r\cos(\theta)\cos(\beta_i) \\ r'_i - r'_{-i} &= r\cos(\theta - \beta_i) - r\cos(\theta + \beta_i) \\ &= 2r\sin(\theta)\sin(\beta_i) \end{aligned}$$

Let:

$$a = \frac{\sum_{i=0/1}^{n} r'_i + r'_{-i}}{\sum_{i=1}^{n} 2\cos(\beta_i)} = r\cos(\theta)$$
$$b = \frac{\sum_{i=0/1}^{n} r'_i - r'_{-i}}{\sum_{i=1}^{n} 2\sin(\beta_i)} = r\sin(\theta)$$

so that:

$$\theta = \arctan(\frac{b}{a}), \quad r = (a^2 + b^2)^{\frac{1}{2}}$$

which exploits the trigonometric identity $A\cos^2(x) + A\sin^2(x) = A$. The initial term of the sums for a and b is 0 if n is odd (center sensor should be included) and 1 if n is even.

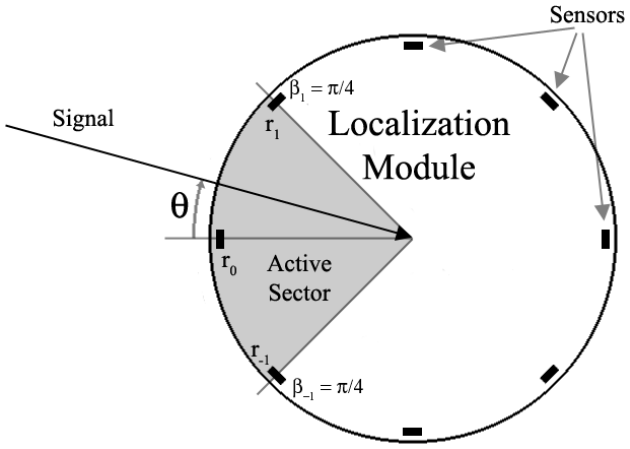

Fig. 3. Relative Positioning Module Receiving Signal

We can apply this algorithm to our current system. With some empirical trials, we determined that the best accuracy was obtained using three of the eight total sensors. Given the signal strength at all infrared receivers, we can find the sector of three sensors with the strongest total received signal; this provides us with the values r'_{-1}, r'_0, and r'_1. In this system, $\beta_1 = \frac{\pi}{4}$, and thus:

$$r'_{-1} = r\cos(\theta + \frac{\pi}{4}), \quad r'_0 = r\cos(\theta), \quad r'_1 = r\cos(\theta - \frac{\pi}{4})$$

Based on this, we get the formulas:

$$a = \frac{r'_1 + r'_{-1} + 2r'_0}{2\cos(\frac{\pi}{4}) + 2}, \quad b = \frac{r'_1 - r'_{-1}}{2\sin(\frac{\pi}{4})}$$

which we can use to get:

$$\begin{aligned} \theta &= \arctan(\frac{b}{a}), \quad r = (a^2 + b^2)^{\frac{1}{2}} \\ \phi &= \text{quadrant angle} + \theta \end{aligned}$$

where ϕ specifies the bearing and r can be converted into range using a lookup table.

V. Module Characterization

The required accuracy of a relative positioning system is highly dependent upon its application; a loose flocking algorithm might require ranging accuracy on the order of tens of centimeters and bearing accuracy on the order of radians, while a precise formation application might need range and bearing accuracies of centimeters and degrees, respectively. In order to effectively judge the accuracy of our positioning system, a thorough characterization of its responses at different ranges and bearings is necessary.

The overhead camera positioning system described in [22] was used to provide ground-truth measurements of robot positions during characterization; a "hat" with a red square and a blue square is attached on top of each robot in order

to calculate their position and bearing. The precision of the system is 15 mm accuracy in positioning and 2.6° accuracy in bearing. This is significantly smaller than the step sizes in our experiments, and we henceforth consider measurements by the overhead camera system as the actual positions and angles of the robots.

For all experiments here, we use the highest power setting on our relative positioning module.

A. Range Term vs Distance

To convert the calculated range term r into a distance, it is necessary to manually measure range terms at different distances to create an accurate lookup table. Using the algorithm previously described, we used two robots to create this table, which is graphically depicted in Fig. 4. We assume that the minimum range possible is 20 cm, as the RSSI reaches its maximum value around this distance. The RSSI drops off rapidly as distance increases up to approximately 60 cm, then gradually decreases up to the maximum range. This results in much more accurate range measurements for small distances, since RSSI variation has less effect here, and less accurate for large distances which are heavily influenced by changing RSSI values.

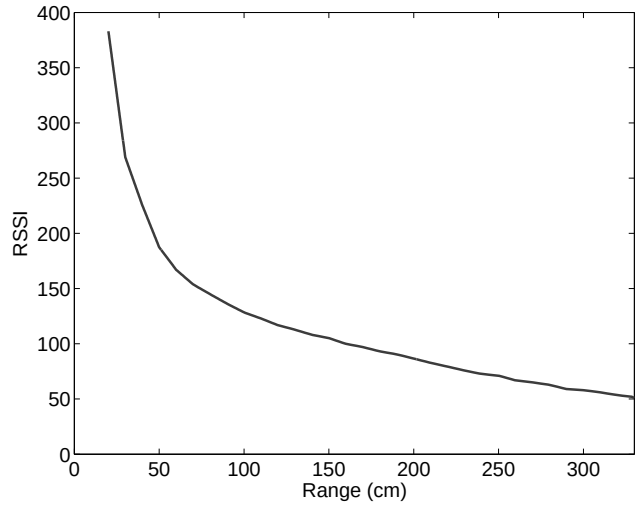

Fig. 4. Calculated Range Term vs. Distance

While measuring range term values, we discovered that different receivers on the relative positioning module could be more or less sensitive, with some giving significantly higher or lower RSSI values for the same signal. In order to compensate for this, we measured the mean RSSI value for each sensor directly facing a transmitting robot at 100 cm range and saved these values on the robot. Using this simple calibration procedure, when calculating range and bearing, the robot uses these values to scale all RSSI measurements, in order to obtain consistency across all receiving channels.

B. RSSI Noise

It is helpful to observe how much noise is present on our measured RSSI values, in order to determine the accuracy limit of our system (i.e. if we have very noisy RSSI measurements, it will be impossible for us to obtain very accurate range and bearing measurements). To do this, we measured the percentage variation in RSSI between two stationary robots for receivers with angular offsets of $-45°$, $0°$, and $45°$. This was done at ranges of 20 cm, 100 cm, and 300 cm. The results can be seen in Fig. 5. The variation in RSSI is quite small in all cases, particularly for ranges of 20 cm and 100 cm, where standard deviation remains below 1%. Variation remains below 5% at a range of 300 cm. Not surprisingly, we see a higher percentage variation for receivers with angular offsets, since these will perceived a smaller signal RSSI and therefore be more sensitive to background noise. The consistency of these measurements implies that, if RSSI variation were the only source of error, we should be able to obtain highly accurate measures of range and bearing even for ranges up to 300 cm.

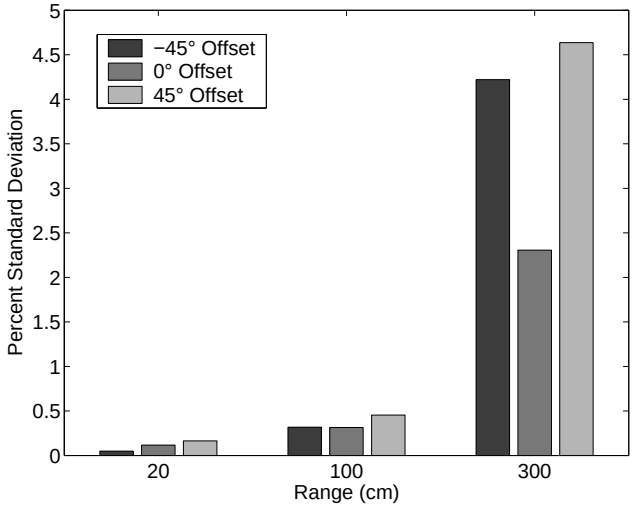

Fig. 5. Standard deviation for 100 RSSI measurements from infrared receivers at different angular offsets and distances

C. Bearing Accuracy

We next explore how much error is actually present in the bearing measurements from the relative positioning module. To do this, we fixed the position of a transmitting robot and moved a receiving robot through 40 different bearings (step size of $9°$) at distances of 20 cm, 100 cm, and 300 cm. We took 100 bearing measurements at each position. The amount of error for different bearings can be seen graphically in Fig. 6 and numerically in Table I. The mean measured bearing generally remains close to actual bearing, though it does vary both above and below. These variations are the result of the angular response of the receiver not exactly matching our model, which introduces error into our calculations. As was suggested by our RSSI variance measurements, the standard deviation of the bearing at a fixed pose is very small in almost all cases.

D. Range Accuracy

We now study the accuracy of the distance measurements given by the range term using the previously described lookup

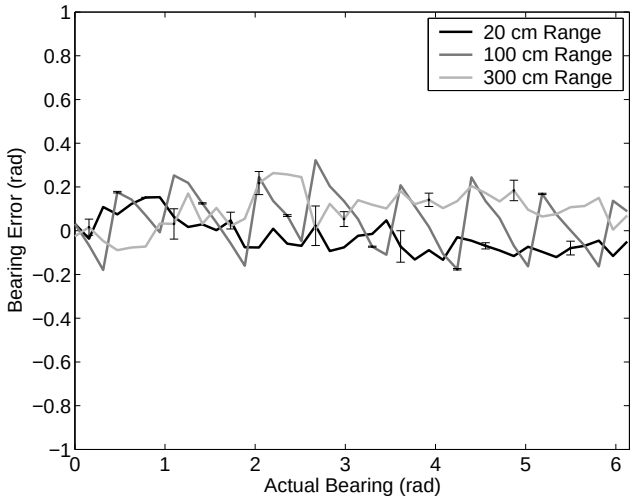

Fig. 6. Bearing error vs. actual bearing for ranges of 20 cm, 100 cm, and 300 cm. 100 measurements were taken at each position. Angles are shown in radians. Error bars represent standard deviation.

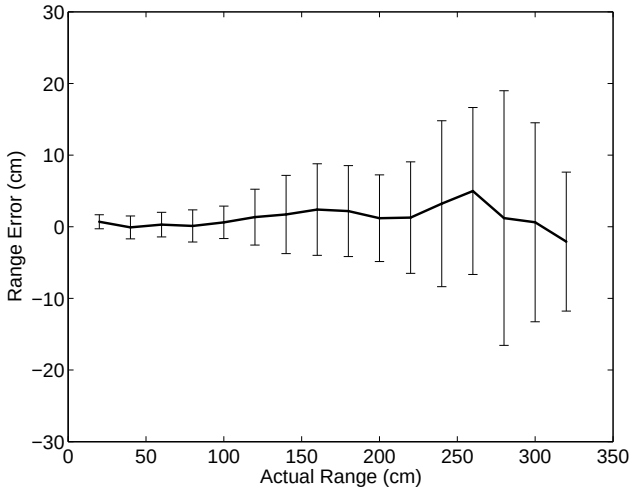

Fig. 7. Measured range vs. actual range averaged across 40 different angular positions at each distance. 100 measurements were taken at each position. Error bars represent standard deviation.

TABLE I
BEARING CHARACTERIZATION ERROR

Distance	RMS Error	Max Error	RMS Std. Dev.	Max Std. Dev.
20 cm	4.64°	8.77°	1.43°	5.17°
100 cm	8.25°	19.0°	0.188°	0.290°
300 cm	7.39°	15.1°	2.78°	6.93°

table. We again fixed the position of a transmitting robot and moved a receiving robot through 40 different bearings (step size of 9°) at 16 distances between 20 cm and 320 cm (step size of 20 cm). For each range, we observe the mean and standard deviation of the measured range across all bearings, with 100 measurements at each bearing. The results are shown in Fig. 7. The average measured range is quite close to the actual range in all cases: the maximum mean distance deviation is 4.99 cm at 240 cm range, and the maximum mean range percentage deviation is 3.48% (0.69 cm) at 20 cm range. This deviation is significantly smaller than that observed for bearing measurements; the reason for this is that the inaccuracies in our model of the receiver angular response has a much higher impact for bearing calculations than range calculations. The standard deviation in range is very low for small ranges, but increases for larger distances: the maximum distance error (and range percentage error) is 18.4 cm (6.56%) at 240 cm range. This is because for larger ranges, even minor variations in the range term cause significant variations in measured range.

E. Transmitter Error

Thus far we have only run experiments using a stationary transmitting robot. An additional source of error could be variation in emission power for different bearings of the transmitter. While this should not affect bearing measurements, it could potentially cause significant changes in the measured range. To explore this possibility, we fix the position of a receiving robot and move a transmitting robot through 40 different bearings (step size of 9°) at distances of 30 cm, 100 cm, and 300 cm (we choose 30 cm instead of 20 cm here in order to observe both positive and negative range variations). The variation is range is shown in Fig. 8. We see that the angle of the transmitting robot does have a significant effect on the measured range; the standard deviation across all angles is 1.87 cm (6.23%) at 30 cm, 8.25 cm (8.25%) at 100 cm, and 17.8 cm (5.92%) at 300 cm. Error caused by transmitting bearing is therefore more significant than receiver error, although still only a small percentage of the total range.

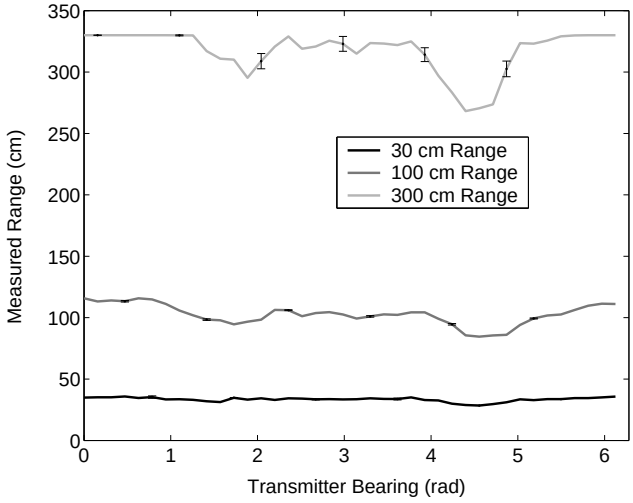

Fig. 8. Measured range vs. transmitter bearing for ranges of 30 cm, 100 cm, and 300 cm. 100 measurements were taken at each position. Angles are shown in radians. Error bars represent standard deviation.

F. Dynamic Range Error

All experiments thus far have measured the accuracy of our relative positioning model in static arrangements where neither the receiving nor the transmitting robot were moving. In actual experiments, it is much more likely that robots will need to be moving while doing relative positioning. To assess

the accuracy of this dynamic positioning, we run a simple experiment in which one robot must follow another.

In this experiment, one leader robot continuously moves forwards and backwards in a straight line of length 30 cm at a speed of 10 cm/s. A second robot begins at a distance of 60 cm from the leader robot, facing the opposite direction, and attempts to maintain a constant distance to the leader using its relative positioning measurements (see Fig. 9). The follower robot is constrained to only move forwards or backwards with no turning allowed. We use a simple controller in which the follower velocity is proportional the measured distance error.

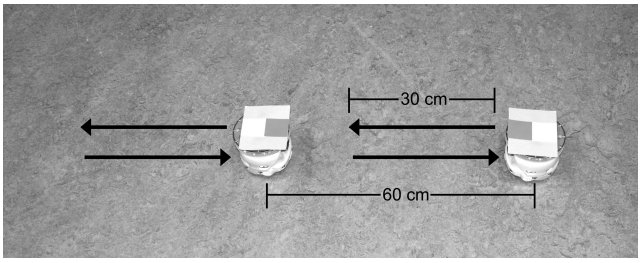

Fig. 9. Dynamic range error experimental setup, with leader and follower robot making repeated identical short steps back and forth. Leader robot is shown on the left.

The performance for the dynamic range experiments over five minutes can be seen in Fig. 10. To contrast the results of the following robot using relative positioning (Leader-Follower), we also display results for both robots running the fixed forwards/backwards motion. We observe that in the open-loop Leader-Leader case, where both robots use identical behavior but have no way to correct for cumulative errors from wheel slip, the error in distance continuously grows throughout the experiment. In contrast, for the closed-loop Leader-Follower case, the error remains relatively low and constant throughout the experiment, as the follower robot is able to maintain the appropriate distance using the relative positioning board. The maximum error is approximately 5 cm, which is similar to the level observed in the static case, indicating that we do not suffer a significant decrease in system accuracy for dynamic experiments.

The comparison here between our open-loop fixed motion controller and our closed-loop relative positioning system is not particularly fair, as a closed-loop systems will always outperform an open-loop systems if enough time has passed. However, it does serve to demonstrate how quickly such a simple behavior can break down without such a system in place.

VI. Multi-Robot Formation Experiments

In order to validate the effectiveness of our relative positioning system, we apply it to the task of multi-robot formation movement. In past studies, using on-board relative positioning resulted in formation which are either very slow (2 cm/s in the case of [8] and approximately 1 mm/s in the case of [26]) or inaccurate (minimum of 20 cm average distance error for robots less than 60 cm apart in [23]). Fast (10 cm/s) formation experiments were more recently performed in [25], but the precise accuracy was not provided. We hope to achieve

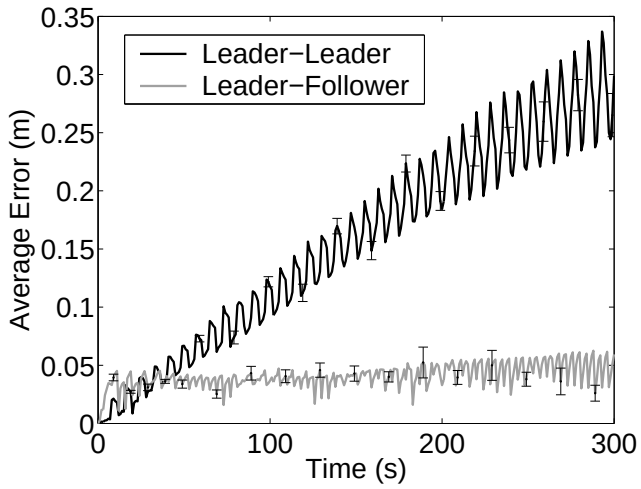

Fig. 10. Error in distance for dynamic range error experiments using two robots running in open-loop mode (Leader-Leader) or one robot following the other in closed-loop mode (Leader-Follower). Results are averaged over 10 runs. Error bars represent standard error.

fast, accurate formation movement using our new relative positioning system.

By itself, our relative localization system can only allow some robot A to detect the range and bearing of another robot B, not the relative direction in which B is facing. This limitation can be overcome if we introduce high-speed communication between the robots. The relative positioning observation of robot B can be sent to robot A, which will allow A to determine B's heading. While the data rate of the current relative localization system's communication is sufficient to accomplish this, it would yield a slower update rate than regular relative positioning, as only 16 bits can be sent per packet, which is not enough to accurately describe the robot's observations. We therefore use the much faster on-board IEEE 802.11 wireless interface as our communication channel.

For our formation control algorithm, we use the approach described in [1], with potential field attraction/repulsion for maintaining formation position, combined with obstacle avoidance using a motor schema method.

We consider two different types of robot formations: location-based and heading-based. In location-based formations, we care about robot positions in the formation and ignore the different directions which robots may be facing. In heading-based formations, robots are required to maintain a certain position and heading for the formation to be correct. It is only possible to implement heading-based formations with robots that can detect the headings of neighboring robots, making them more difficult to maintain. We consider the further subcategory of leader heading-based formations, where follower robot locations are determined by the position and heading of the leader, but the headings of the followers are ignored.

A. Experimental Setup

Four robots are placed in a diamond shape in an arena measuring 3.4 m x 3.4 m. All robots are offset 0.4 m from

the center of the formation, and the leader robot (the one at the front of the formation) travels an elongated figure 8 path around the arena (see Fig. 11). With four robots transmitting simultaneously, we observed a relative positioning update rate between 15 Hz and 20 Hz for each robot. However, the main loop of the robot only executed at approximately 10 Hz, effectively limiting the relative positioning update to this rate. We use the previously mentioned overhead camera localization system to track the location and bearing of the robots. A close-up of the real robot formation is shown in Fig. 12. Robots operate in three different modes:

Mode 1: No Relative Positioning - The follower robots are preprogrammed with the course they must take to maintain formation with the leader robot. There is no feedback to compensate for robot drift due to wheel slip or motor inaccuracies.

Mode 2: Relative Positioning Without Communication - The on-board relative positioning module is used to detect the range and bearing of other robots in the formation. Position is maintained by using a potential field approach to keep the proper distance to all other robots. In order to keep pace with the leader robot, the potential field of the leader is given twice the weight of the other robots. Additionally, we attempt to do primitive speed matching with the leader robot by scaling the desired range (r_{target}) at each step of the algorithm by ratio of the default desired range (r_{def}) to the range at the previous step (r_{prev}): $r_{target} = r_{def} \frac{r_{def}}{r_{prev}}$.

Mode 3: Relative Positioning With Communication - The on-board relative positioning module is used along with wireless communication to allow robots to detect the range, bearing, and heading of other robots. Position is maintained by using the potential field approach to move to the proper position based on the location and heading of the leader.

Comparing to previous formation-maintaining techniques, the methods used in Mode 2 and Mode 3 are roughly the equivalent of Unit-center-referenced and Leader-referenced methods described in [1], respectively.

Our first experiment compares Mode 1 and Mode 2 running with a location-based formation, and our second compares Mode 2 and Mode 3 running with a leader heading-based formation. Mode 2 is well-suited for location-based formation, since it maintains the proper distances between teammates, but not for leader heading-based formation, since it ignores the heading of the leader; Mode 3 is well-suited for leader heading-based formation, since it takes the leader heading into account. The leader robot moves at 10 cm/s, which allowed it to completely traverse the figure eight path in 95 seconds. Experiments were run for 120 seconds.

B. Results

Comparison between Mode 1 and Mode 2 for location-based formation can be seen in Fig. 13. The error given here is the average error in distance between robots in the formation (averaged over all six edges between the four robots). Initially, Mode 1 is able to maintain a better formation than Mode 2, since the error due to slip noise accumulates over time, but it very quickly surpasses the error of Mode 2, which remains quite low throughout the experiment at approximately 10 cm. This is approximately 50% of the average error that was obtained in [23] and is similar to the predicted error for a relative positioning system with a faster update rate of 16 Hz.

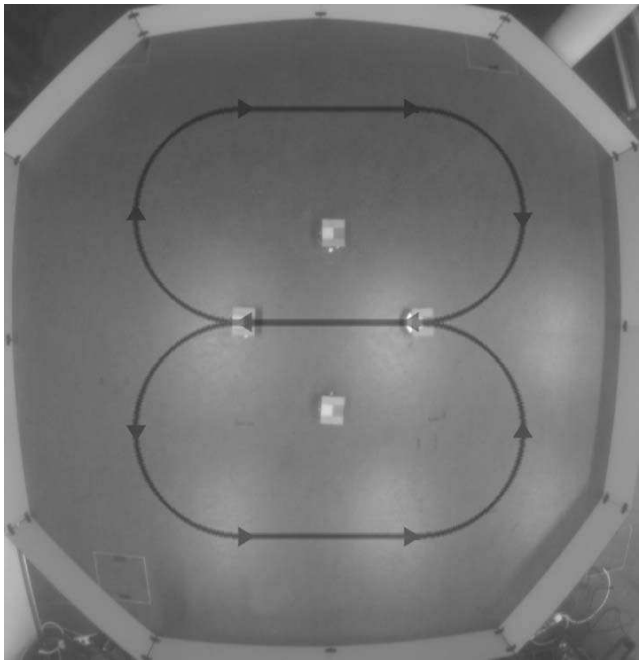

Fig. 11. Picture of arena taken by overhead tracking camera with Khepera III robots in initial formation positions. The path of the formation leader is shown.

Fig. 12. Formation of Khepera III robots

If we compare the distance error from the formation (approximately 10 cm) to the characterization error for 60-80 cm in the previous section (approximately 3 cm), we observe a substantial increase. While some of this may be the result of transmission variation error, much of it is likely caused by the formation control technique used; because the potential field "force" applied to a robot is proportional to the position error, it will be slow to respond until its position error becomes significant. This was already partially observable in the dynamic range error test and is even more visible here, due to the difficult turns performed by the leader robot.

As in the dynamic range error experiment, matching up our open-loop fixed motion controller against our closed-

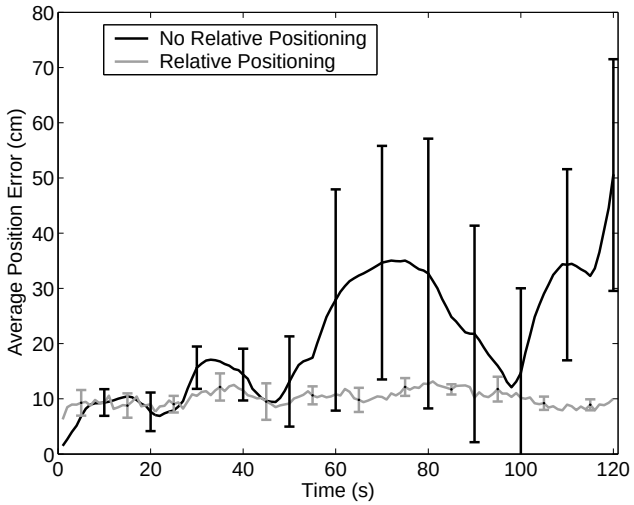

Fig. 13. Average error in position for location-based formation over 10 runs. Error bars represent standard deviation.

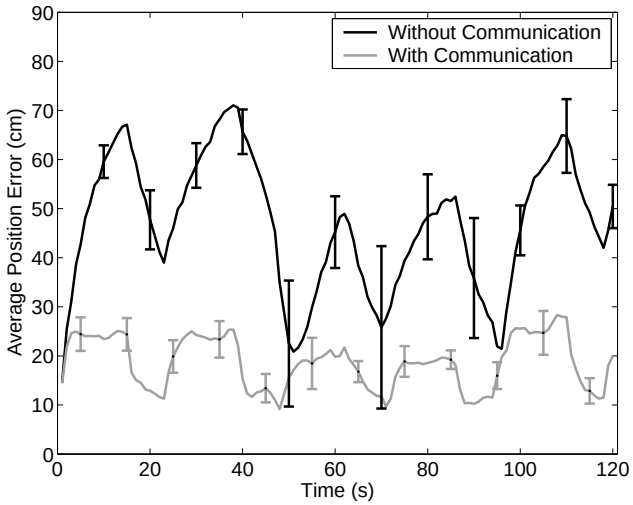

Fig. 14. Average error in position for leader heading-based formation over 10 runs. Error bars represent standard deviation.

loop relative positioning system is not a fair comparison, as a closed-loop systems will always eventually outperform an open-loop systems. It is interesting to observe that the open-loop system performs comparably to the closed loop system for the first 20 seconds of the experiment, however. This suggests that a hybrid approach might be employable, where followers use a pre-programmed course, and only correct their position when error grows too large.

Comparisons between Mode 2 and Mode 3 for leader heading-based formation can be seen in Fig. 14. The error for Mode 2 is significantly higher for leader heading-based formation than for location-based formation, as the robots are unable to detect the heading of the leader robot. Mode 3 is able to achieve much better performance than Mode 2, although the error is still higher than for location-based formation, varying between 10 cm and 25 cm. This is not too surprising, however, when one considers how much error is introduced by only small rotations of the leader; a 20° rotation will already cause 22.5 cm of error. The oscillations in the error are caused by the periodic turns of the leader, where the follower robots must respond and move very quickly to keep up. Once the leader stops turning, the followers quickly regain their proper positions.

VII. Discussion and Outlook

In characterizing the accuracy of our relative positioning system, we observed that the bearing error was significantly increased by the inaccuracy of our model for the angular response of the infrared photo-diodes, which often varied significantly between different photo-diodes. An alternative approach that could potentially overcome this problem is to run a full calibration of all photo-diodes at different angles with different signal intensities and record their responses. This could be used to create a giant lookup table which could be used to very accurately determine bearing (and range) in all situations. However, a characterization of that magnitude would be extremely time-consuming, and the resulting lookup table might be too large to be stored on simple robots. It is possible that a sparser lookup table could offer improved performance without the need for extensive calibration and storage space, though this would need to be verified.

While the error due to receiver angular response inaccuracy could be removed using calibration, this is not possible for error due to varying emission power from different transmitter bearings, as receiving robots have no way of determining the bearing of the robot which is broadcasting. The only way to overcome this is to ensure that all transmission sectors on the relative positioning modules emit equal power. This could be accomplished by either (a) adding some device which could be used to precisely adjust the output power (i.e. a potentiometer), or (b) only using components which are guaranteed (either by the manufacturing or via hand selection) to give consistent response. Alternatively, the system could be redesigned to use only a single emission source which is projected omnidirectionally using a conical mirror, although this would likely result in a considerably more bulky module with less flexibility, as we would no longer have control over emission directionality by enabling or disabling different sectors.

All experiments in this work were performed on a smooth, indoor arena without any unevenness that could alter the yaw of the robots. If experiments were to be run on a rough terrain, the relative positioning error would be increased, as angled LEDs and photo-diodes would cause both emission and reception strength to be attenuated, resulting in inaccurate measurements. If operation on uneven terrain were required, this limitation could be overcome by using wider emission angle LEDs (current LEDs have a half-power angle of 30°) and two rows of photo-diodes with positive and negative yaw offsets; this would allow for the explicit calculation of the relative yaw of the receiving robot, which could then be accounted for in the range and bearing calculations. A similar approach could potentially be used for flying/underwater vehicles, allowing for relative positioning in three dimensions instead of two.

Although it was not explored here, the presented relative po-

sitioning system could potentially be used for effective control of highly dynamic robot formations, where groups of robots need to quickly change from one configuration to another. This behavior is useful in many of the applications where multi-robot formations are required (e.g., adaptive collective transport). The suitability of this system for such behavior should be further explored.

VIII. Conclusion

We have presented a state-of-the-art on-board relative positioning module for mobile miniature robots which operates using modulated infrared signals. A general technique for calculating the range and bearing between robots for RSSI-based systems has been described and applied specifically to our module. We have fully characterized the performance and accuracy of the module and identified the probable causes of imprecision. The system has been shown to enable fast, accurate multi-robot formation movement in several modalities without global positioning and is a significant improvement over existing work reported in the literature.

IX. Acknowledgements

This work has been mainly sponsored by a Swiss NSF grant (contract Nr. PP002-116913).

References

[1] Balch, T. & Arkin, T. C., (1998) “Behavior-Based Formation Control for Multirobots Teams”, IEEE Trans. on Robotics and Automation, Vol. 14, No. 6, pp. 926-939.

[2] Balch, T. & Hybinette, M. (2000) “Social Potentials for Scalable Multi-Robot Formations”, Proc. of the IEEE International Conference on Robotics and Automation, San Francisco, CA, April, pp. 73-80.

[3] Bergbreiter, S., Mehta, A., & Pister, K. S. J. (2007) “PhotoBeacon: Design of an Optical System for Localization and Communication in Multi-Robot Systems”, Proc. of the International Conference on Robot Communication and Coordination, Athens, Greece, October, Article No. 5.

[4] Bisson, J., Michaud, F. & Létourneau, D. (2003) “Relative Positioning of Mobile Robots Using Ultrasounds”, IEEE Int. Conf. on Robotics and Authomation IROS03, Oct, Las Vegas, Nevada, USA, pp. 1783-1788.

[5] Chen, Q. & Luh, J. Y. S. (1994) “Coordination and Control of a Group of Small Mobile Robots”, Proc. of the IEEE International Conference on Robotics and Automation, San Diego, CA, pp. 2315-2320.

[6] Choset, H. (2001) “Coverage for Robotics - A Survey of Recent Results”, Annals of Mathematics and Artificial Intelligence, Vol. 31, pp. 113-126.

[7] Desai, J. P., Ostrowski, J. P., & Kumar, V. (2001) “Modeling and Control of Formations of Nonholonomic Mobile Robots”, IEEE Trans. on Robotics and Automation, Vol. 17, No. 4, pp. 905-908.

[8] Fredslund, J. & Matarić, M. J. (2002) “General Algorithm for Robot Formations Using Local Sensing and Minimal Communication”, Special Issue on Advances in Multi-Robot Systems, Arai T., Pagello E., and Parker L. E., editors, IEEE Trans. on Robotics and Automation, Vol. 18, No. 5, pp. 837-846.

[9] Fox, D., Burgard, W., Kruppa, H., & Thrun, S. (2000) “A Probabilistic Approach to Collaborative Multi-Robot Localization”, Autonomous Robots, Vol. 8, No. 3, pp. 325-344.

[10] Grabowski, R. & Khosla, P. (2001) “Localization Techniques for a Team of Small Robots”, Proc. of the IEEE/RSJ International Conference on Intelligent Robots and Systems, Maui, HI, Oct 29-Nov 3, pp. 1067-1072.

[11] Hao, Y. & Agrawal, S. K. (2005) “Planning and Control of UGV Formations in a Dynamic Environment: A Practical Framework with Experiments”, Robotics and Autonomous Systems, Vol. 51, No. 2-3, pp. 101-110.

[12] Hashemi, H., Guan, X. & Hajimiri, A. (2004) “A Fully Integrated 24 GHz 8-path Phased-Array Receiver in Silicon”, IEEE Int. Solid-State Circuits Conf. Dig. Tech. Papers, Feb., pp. 318-319.

[13] Hayes, A. T., Martinoli, A. & Goodman, R. M. (2002) “Distributed Odor Source Localisation”, Special Issue on Artificial Olfaction, Nagle H. T., Gardner J. W., and Persaud K., editors, IEEE Sensors Journal, Vol. 2, No. 3, pp. 260-271.

[14] Howard, A., Matarić, M. J., & Sukhatme, G. S. (2003) “Localization for Mobile Robot Teams: A Distributed MLE Approach”, Springer Tracts in Advanced Robotics, Vol. 5, Jan 2003, pp. 146-155.

[15] Hwang, C. L. & Chang, L. J. (2007) “Trajectory Tracking and Obstacle Avoidance of Car-Like Mobile Robots in an Intelligent Space Using Mixed H_2/H_∞ Decentralized Control”, IEEE/ASME Trans. on Mechatronics, Vol. 12, No. 3, pp. 345-352.

[16] Kelly, I. D. & Martinoli, A. (2004) “A Scalable, On-Board Localisation and Communication System for Indoor Multi-Robot Experiments”, Special Issue on Sensor Simulation and Smart Sensors, C. Loughlin, editor, Sensor Review, Vol. 24, No. 2, pp. 167-180.

[17] Lanzisera, S., Lin, D. T., & Pister, K. S. J. (2006) “RF Time of Flight Ranging for Wireless Sensor Network Localization”, Workshop on Intelligent Solutions in Embedded Systems, Vienna, Austria, June, pp. 1-12.

[18] Lawton, J. R. T., Beard, R. W., & Young, B. J. (2003) “A Decentralized Approach to Formation Maneuvers”, IEEE Trans. on Robotics and Automation, Vol. 19, No. 6, pp. 933-941.

[19] Lee, J. Y. & Scholtz, R. A. (2002) “Ranging in a Dense Multipath Environment Using an UWB Radio Link”, IEEE Journal on Selected Areas in Communications, Vol. 20, No. 9, pp. 1677-1683.

[20] Martinoli, A. (1999) “Swarm Intelligence in Autonomous Collective Robotics: From Tools to the Analysis and Synthesis of Distributed Collective Strategies”, Ph.D. Thesis Nr. 2069, October, 1999, DI-EPFL, Lausanne, Switzerland. Downloadable from http://infoscience.epfl.ch.

[21] McLurkin, J. & Smith, J. (2004) “Distributed Algorithms for Dispersion in Indoor Environments using a Swarm of Autonomous Mobile Robots”, Proc. of the Seventh Int. Symp. on Distributed Autonomous Robotic Systems, Toulouse, France, June 23-25, pp. 381-390.

[22] Pugh, J. & Martinoli, A. (2006) “Relative Localization and Communication Module for Small-Scale Multi-Robot Systems”, Proc. of the IEEE International Conference on Robotics and Automation, Miami, FL, May 15-19, pp. 188-193.

[23] Pugh, J. & Martinoli, A. (2008) “Small-Scale Robot Formation Movement Using a Simple On-Board Relative Positioning System”, July 2006, Rio de Janeiro, Brazil, Springer Tracts in Advanced Robotics (2008), Vol. 39, pp. 297-306.

[24] Rekleitis, I., Dudek, G. & Milios, E. (2001) “Multi-robot collaboration for robust exploration”, Annals of Mathematics and Artificial Intelligence, Vol. 31, pp. 7-40.

[25] Rivard, F., Bisson, J., Michaud, F. & Letourneau, D. (2008) “Ultrasonic relative positioning for multi-robot systems”, Proc. of the IEEE International Conference on Robotics and Automation, Pasadena, CA, May 19-23, pp. 323-328.

[26] Spears, W. M., Spears, D. F., Hamann, J. C. & Heil, R. (2004) “Distributed, Physics-Based Control of Swarms of Vehicles”, Autonomous Robots, Vol. 17, No. 2-3, pp. 137-162.

[27] Winfield, A. F. T. & Holland, O. E. (2000) “The application of wireless local area network technology to the control of mobile robots”, Microprocessors and Microsystems, Vol. 23, No. 10, pp. 597-607.

[28] Yamaguchi, H., Arai, T. & Beni, G. (1997) “A distributed control scheme for multiple robotic vehicles to make group formations”, Robotics and Autonomous Systems, Vol. 36, No. 4, pp. 125-147.

[29] Yang, E. & Gu, D. (2007) “Nonlinear Formation-Keeping and Mooring Control of Multiple Autonomous Underwater Vehicles”, IEEE/ASME Trans. on Mechatronics, Vol. 12, No. 2, pp. 164-178.